ACCOUNTS
of chemical research

Theory-Inspired Development of Organic Electro-optic Materials

PHILIP A. SULLIVAN AND LARRY R. DALTON*
Department of Chemistry, University of Washington, Seattle, Washington 98195-1700

RECEIVED ON DECEMBER 1, 2008

CONSPECTUS

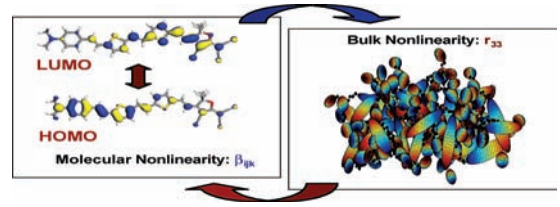

Correlated time-dependent density functional theory (TDDFT) quantum mechanical and pseudo-atomistic Monte Carlo (PAMC) statistical mechanical methods have been used to assist in the understanding of and to guide the improvement of organic electro-optic (OEO) materials, prepared by electric field poling of π-electron chromophore-containing materials near their glass transition temperature. Theoretical treatment of the effects of dielectric permittivity and optical frequency on molecular (chromophore) first hyperpolarizabilities has been carried out as well as the analysis of the influence of spatially anisotropic intermolecular electrostatic interactions on the poling-induced noncentrosymmetric order of chromophores. Three classes of OEO materials have been considered in correlated theoretical and experimental investigations: (1) traditional chromophore/polymer composite materials, (2) chromophores covalently incorporated into polymers, dendrimers, and dendronized polymers, and (3) recently discovered materials consisting of chromophores incorporated into chromophore-containing host materials. This latter class of materials is referred to as binary chromophore organic glasses (BCOGs). These BCOGs exhibit exceptional electro-optic activity because of a combination of high chromophore number density, the effect of high dielectric permittivity on molecular first hyperpolarizability, and improved acentric order arising from the intermolecular electrostatic interactions among the two types of chromophores. The electrical conductivity of materials can also influence achievable electro-optic activity, and thin metal oxide buffer layers, introduced to limit charge injection, can significantly improve poling efficiency. Chromophore order can also be influenced, in some cases, by novel processing techniques, such as laser-assisted electric field poling. Thermal and photostability are important parameters for practical application of materials and have been improved dramatically in recent times. Diels–Alder and fluorovinyl ether cycloaddition reactions have been used to elevate final material glass transition temperatures to above 200 °C. Photostability is dominated by the photoactivation of singlet oxygen and subsequent attack on electro-optic chromophores. Photostability can be improved by more than 4 orders of magnitude by chromophore modification and material packaging.

Introduction

In telecommunications, computing, and sensing, interconversion between "electronic" and "photonic" signal domains has become increasingly important with time. A motivation for the increasing use of photons as the carrier of information is the resistive losses that occur with electrons moving through metal wires, which are increasingly problematic as the frequency of information increases. In addition to current widespread use in long-distance fiber-optic networks, photonic solutions are increasingly being implemented for information transport over ever shorter distances; e.g., chipscale integration of photonics and electronics has become an important objective in both civilian (computing, telecommunication, transportation, and medicine) and defense sectors. This most recent evolution is driven by the fact that higher frequency content of information generated in computing or by sensors is rapidly growing. Additionally, thermal management and electrical crosstalk are ever increasing problems as the density of active elements on chips increases. Use of photons affords enormous advantages rel-

Published on the Web 08/07/2009 www.pubs.acs.org/acr
10.1021/ar800264w

ative to the use of electrons for improved thermal management and reduced crosstalk.

The ability to convert signals between electronic and photonic domains is central to photonic/electronic integration. Materials and devices that effect such transduction are referred to as "electro-optic" (or EO). Electrical-to-optical signal transduction has been achieved in the past by use of a number of technologies, including thermo-optic devices, liquid crystals, and inorganic EO crystals. Because of fundamental response time limitations imposed by physical temperature change (thermo-optic) and molecular motion (liquid crystals), these technologies are not appropriate for high-frequency (bandwidth) applications. With ionic crystals, response times are shorter because of the smaller (ion) mass moved in response to the applied electric field; however, the magnitude of the induced phase shift is relatively small (30 pm/V for lithium niobate), requiring a high device drive voltage. In contrast, the EO response of organic π-electron materials is very fast (femtoseconds), and through continuing research efforts, the magnitude of the response is being increased rapidly (to a current value of approximately 500 pm/V). Clearly, organic electro-optic (OEO) materials are of great interest for applications requiring high bandwidth (ultra-fast response times). In addition to electrical-to-optical transducers, optical switches, optical gyroscopes, optical phased array radar, RF (radiofrequency, microwave, and millimeter wave) photonics, ultra-fast A/D and D/A converters, etc., a number of sensing and spectroscopy (e.g., THz spectroscopy) applications requiring ultra-high bandwidth have also motivated the development of new high-performance EO materials.

A material EO activity of $r_{33} = 500-1000$ pm/V, together with the optical loss of less than 2 dB/cm, is an important benchmark for these current and emerging applications; other material properties that are important include adequate thermal and photochemical stability together with good processability and compatibility with diverse materials (metals, silicon, silica, organic cladding materials, etc.). The electrical conductivity of active EO materials can also be important because this can influence the efficiency of electric field poling in the development of materials and bias voltage drift in the operation of devices prepared from OEO materials.

Throughout much of the 1990s, OEO activity hovered around 15 pm/V but, for the past decade, has been increasing at a rate faster than that of Moore's law. The reason for this rate of improvement is theory-inspired design discussed in the next section.

Theory-Inspired Design

The computational approach that has helped to enable the rapid improvement of OEO materials uses coupled (interdependent) statistical and quantum mechanical methods to assess the relationship between bulk and molecular level nonlinear optical (NLO) effects. The principle element of the EO tensor (r_{33}) can be related to the chromophore nonlinearity (first molecular hyperpolarizability $\beta_{zzz}(-\omega; 0, \omega)$) by[1]

$$r_{33}(\omega) = \frac{2N\beta_{zzz}(-\omega;0,\omega)g(\omega)\langle\cos^3\theta\rangle}{n_\omega^4} \qquad (1)$$

where N represents the chromophore number density and $g(\omega)$ denotes the Lorentz−Onsager local field factors. The term $\langle\cos^3\theta\rangle$ is the orientationally averaged acentric order parameter characterizing the degree of noncentrosymmetric alignment of the chromophores in the material with the laboratory z axis (the direction of the electric poling field used to induce noncentrosymmetric order and, also, the direction of the principal axes of the applied optical and electrical fields in operation of devices). The refractive index at the operational frequency, ω, is represented by n_ω. Finally, the dominant molecular first hyperpolarizability tensor element is $\beta_{zzz}(-\omega; 0, \omega)$.

As eq 1 suggests, to theoretically predict r_{33}, not only must $\langle\cos^3\theta\rangle$ be accurately described, but all of the relevant linear and nonlinear optical susceptibility tensor components and their corresponding frequency dependence must be modeled. The material dielectric constant, ε, must be considered either to build an accurate computational model or to design improved materials. In addition to the well-known dependence of $\langle\cos^3\theta\rangle$ on N, ε also depends upon N and the ability of the chromophores to reorient in response to an applied field. Because $\beta_{zzz}(-\omega; 0, \omega)$ exhibits a pronounced dependence upon the dielectric permittivity, quantum mechanical calculations of $\beta_{zzz}(-\omega; 0, \omega)$ must explicitly consider ε.

Modeling of Molecular Linear and Nonlinear Properties. Density functional theory (DFT) allows for the direct calculation of the β tensor via the finite field method. Trends in hyperpolarizability calculated by DFT compare favorably to those from other methods[2] and have been shown to predict experimental trends accurately,[3−5] In addition, DFT is less computationally intensive than other methods and can be readily extended to include time dependence (TDDFT), allowing of the investigation of frequency dispersion effects, and reaction fields, allowing for the investigation of solvent/dielectric environmental effects.[6]

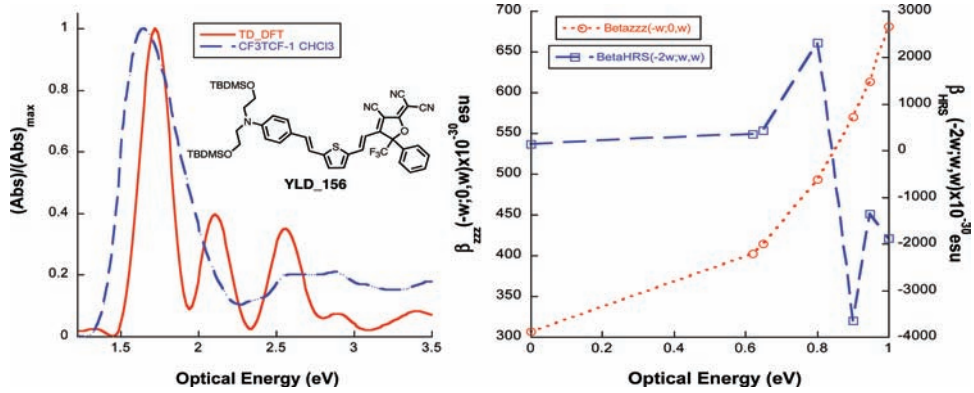

FIGURE 1. Absorption spectrum of YLD_156 simulated using TDDFT (—) overlaid with that measured (- - -) in chloroform solution (left) and the frequency dispersion behavior of $\beta_{zzz}(-\omega; 0, \omega)$ (○, electro-optic effect) and $\beta_{zzz}(-2\omega; 0, \omega)$ (□, second harmonic generation) (right).

The two-level model (TLM) of Oudar and Chemla[1,7] provides a simplistic method of evaluating the frequency dependence of β.[1,8] To select the most appropriate methods, we have compared real-time, time-dependent DFT (RT-TDDFT) to the results from linear-response DFT (lr-DFT) and Hartree−Fock (HF) along with the TLM.[9] The results suggest that the TLM usually provides a simple and useful estimate of frequency dependence at frequencies significantly lower than molecular resonances (ω_{eg}). However, despite moderately high computational expense, the RT-TDDFT technique also allows for the prediction of the real and imaginary parts of the polarizability (α_ω), which is useful for understanding optical loss and other linear optical effects.

Figure 1 illustrates the results obtained from RT-TDDFT for the EO chromophore YLD_156 (2-[4-(2-{5-[2-(4-{bis-[2-(tert-butyl-dimethyl-silanyloxy)-ethyl]-amino}-phenyl)-vinyl]-thiophen-2-yl}-vinyl)-3-cyano-5-phenyl-5-trifluoromethyl-5*H*-furan-2-ylidene]-malononitrile). The left panel shows an overlay of computed and experimentally measured (chloroform solution) absorption spectra, which are in good agreement. The right panel shows the frequency dependence of hyperpolarizability values. Both $\beta_{zzz}(-\omega; 0, \omega)$, the quantity that governs the EO effect (r_{33}), and $\beta_{HRS}(-2\omega; \omega, \omega)$, the quantity associated with second harmonic generation [as measured by hyper-Rayleigh scattering (HRS)[10,11]], are shown. The inflection behavior in $\beta_{HRS}(-2\omega; \omega, \omega)$ centered around $\omega_{eg}/2 \approx 2\lambda_{max}$ illustrates the complication associated with the quantitative comparison of SHG-derived $\beta_{HRS}(-2\omega; \omega, \omega)$ with $\beta_{zzz}(-\omega; 0, \omega)$ required for r_{33}. However, SHG-based measurements can serve as a validation of theoretically derived values.[4,8,12]

To predict r_{33}, the dependence of $\beta_{zzz}(-\omega; 0, \omega)$ on ε must also be understood. Currently, efforts are underway to modify RT-TDDFT methods to simultaneously consider dielectric and frequency dependence. However, at present, the assumption must be made that the two effects may be considered independently and later combined. Dielectric effects can then be estimated using static DFT codes (Dmol[3] PBE/DNP/COSMO).[6,13] From simulation, it is apparent that β_{ijk} varies by up to 4-fold from the gas phase to the solution/solid state.[9] This effect is illustrated in Figure 2, comparing calculated $\beta_{HRS}(0)$ values for YLD_156 to those measured using HRS as a function of solvent ε.

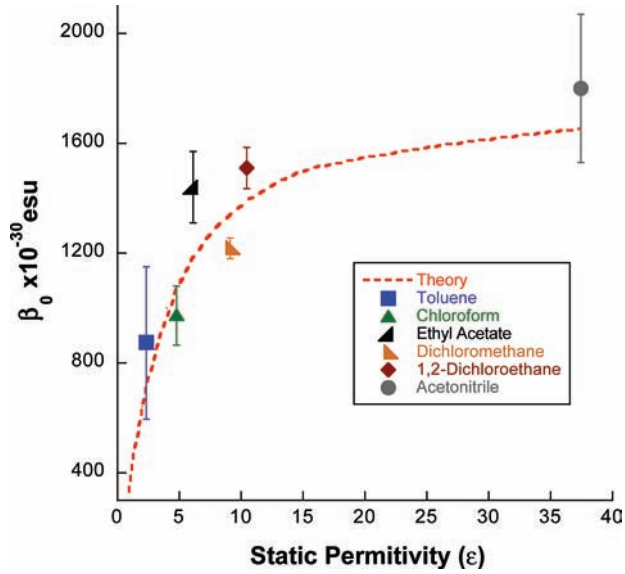

FIGURE 2. Comparison of calculated $\beta_{HRS}(0)$ values for YLD_156 to those measured by HRS (corrected for frequency dispersion assuming a TLM) in different solvents.

Simulation of Poling Induced Order: Pseudo-Atomistic Monte Carlo (PAMC). Sterically modified materials, such as dendrimers,[12,14,15] dendronized polymers,[16,17] and self-assembled materials,[18,19] are all examples of the use of molecular engineering to stabilize or facilitate acentric molecular order. To establish effective theoretical guidance, fully atomistic computer simulations are attractive.[20] It has been previously shown that such simulations must explicitly consider all relevant internal and external potentials, including dipole−

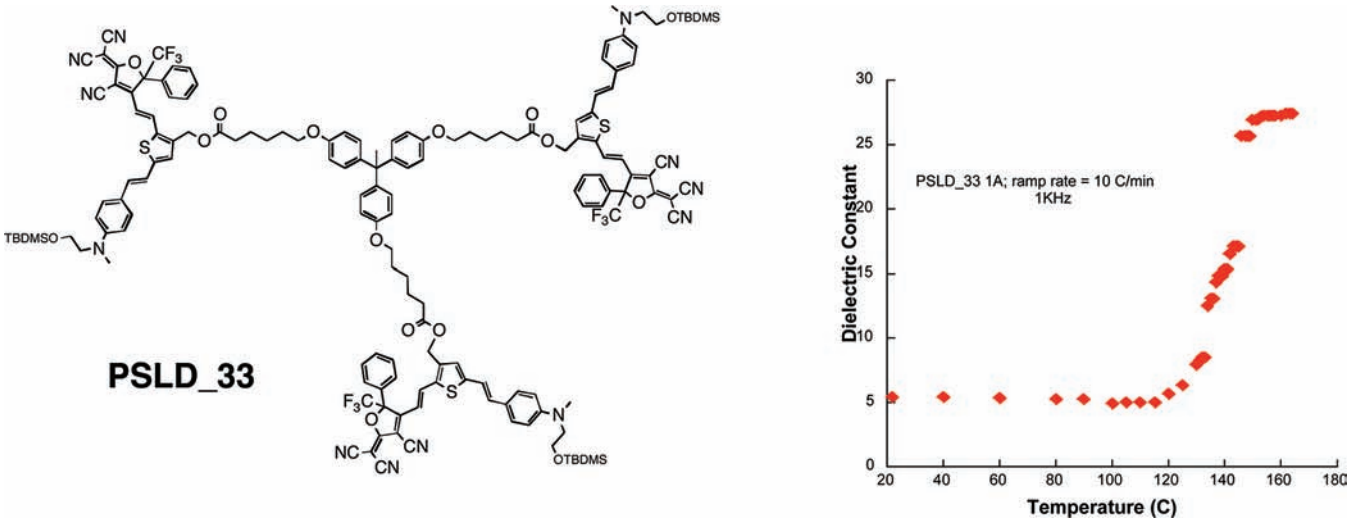

FIGURE 3. (Left) Chemical structure of the PSLD_33 dendrimer is shown. (Right) Experimental temperature dependence of ε is shown.

dipole electrostatic interactions (i.e., orientational pair correlation).[21] To reduce prohibitive computational expense, we have developed PAMC methods. The specific details of the simulations are presented elsewhere.[12,22] The fundamental basis of the "pseudo-atomistic" approach is to treat π-conjugated molecular segments as rigid.

This united-atom approximation allows for the π-conjugated segments of the active EO chromophore to be treated as a dipolar spheroid (ellipsoid). Quantum simulations are used to define the magnitude and distribution of the relevant dipole vectors. σ-bonded segments, such as tethers, dendritic units, or other elements important in defining inter- and intramolecular interactions, are then treated fully atomistically. In addition to the obvious utility of PAMC methods for simulating poling induced order, this method is also valuable for estimating ε. As is evident from the work of Kirkwood, Onsager, and Debye, mobile dipoles able to respond to an applied field will greatly enhance the dielectric constant of the medium.[23,24] Under poling conditions, the contribution from mobile dipoles will dominate the dielectric response. Here, PAMC methods provide a valuable tool with which to assess this dipolar contribution by calculating $\langle\cos^n\theta\rangle/E_p$, where $n =$ 1, 2, or 3. With this term in hand, Onsager's expression may be modified to the form

$$\varepsilon_{tot} - 1 = 4\pi\left(N\frac{\mu}{E_{pol}}\langle\cos\theta\rangle + N_s\frac{f_{LL}\mu_s^2}{3kT}\right) + \sum_{k=1}^{2}\frac{3\varepsilon_{tot}(n_k^2 - 1)}{2\varepsilon_{tot} + n_k^2}\phi_k \quad (3)$$

which is similar to that of Kirkwood.[23]

Applying this approach to the dendrimer system PSLD_33 (Figure 3), by inputing the values of $\langle\cos\theta\rangle/E_p$ calculated from PAMC simulations, together with results for α_ω and thus, η_k, from TDDFT into eq 3, results in a value of $\varepsilon_{tot} \approx 25$. As the PSLD_33 sample is heated above T_g and the dipoles become free to rotate and move, a limiting value of $\varepsilon \approx 27$ is measured experimentally.

Measurement of the Order in Poled Organic EO Material Thin Films. No known methods exist for the direct measurement of either $\beta_{zzz}(-\omega; 0, \omega)$ or $\langle\cos^3\theta\rangle$ in the solid state. However, a polarized absorption spectroscopy (PAS) method to evaluate the centrosymmetric order parameter, $\langle P_2(\cos\theta)\rangle = (1)/(2)(3\langle\cos^2\theta\rangle - 1)$, has been proposed by Graf et al.[25] In this method, a poled sample is placed on a rotation stage that is located within the sample chamber of a UV−vis spectrophotometer modified to include polarization optics. Absorbance as a function of the polarization of the light (s or p) and the angle at which the light enters the sample, θ, is then experimentally determined. The average absorbance of light of frequency $\tilde{\nu}$, polarized parallel to the poling axis (p-polarized), $\langle\alpha_f(\tilde{\nu})\rangle_p$, depends upon the angle at which the light propagates within the EO layer, ψ, by

$$\langle\alpha_f(\tilde{\nu})\rangle_p = \bar{\alpha}_f\{(1 - \langle P_2\rangle) + 3\langle P_2\rangle\sin^2\psi\} \quad (4)$$

where $\bar{\alpha}_f$ is the absorbance of an unpoled sample at normal incidence. Accurate analysis of experimental data requires precise knowledge of the orientation of the optical propagation vector with respect to the poling axis (to determine the relationship between θ and ψ). Additionally, the loss of optical intensity because of reflections at sample interfaces must be quantified. To accomplish this, Graf et al. proposed that the real and imaginary components of the refractive index be treated independently. Through application of Snell's law and approximate correction for interface reflections according to

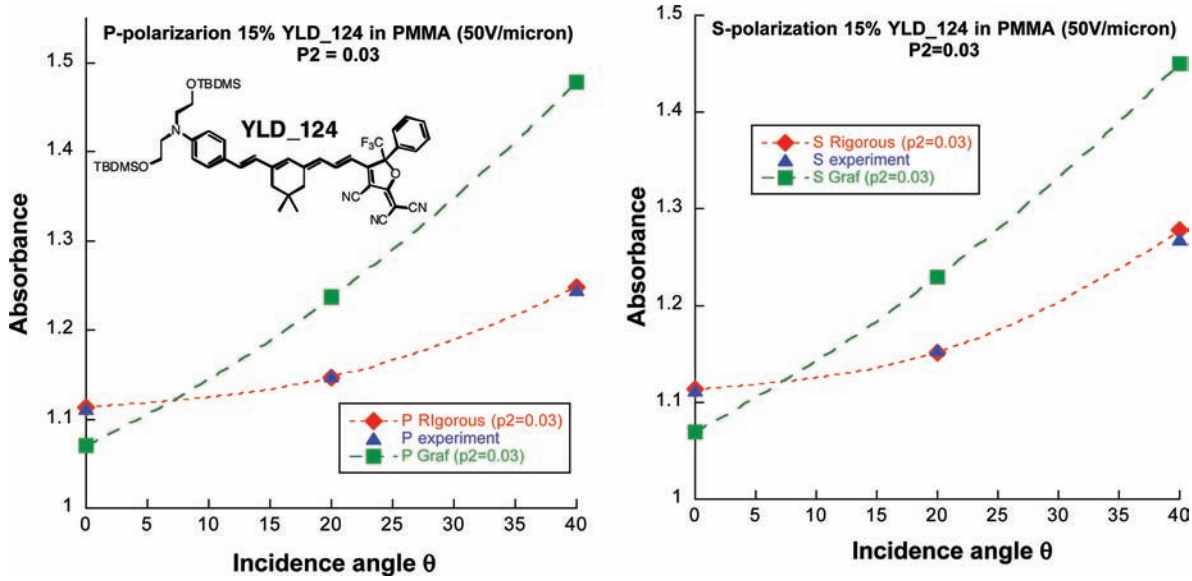

FIGURE 4. (Left) Chemical structure of YLD_124, experimental data (blue triangles) corresponding to the angle-dependent absorption of p-polarized light plotted versus the rigorous model of Mansuripur (red diamonds) and the Graf method predictions (green squares) for a sample 0.95 μm thick of 15% by weight YLD_124 in PMMA poled at 50 V/μm. (Right) Analogous plot of data for s-polarized light taken from the same sample.

Fresnel, the remaining angle dependence of the sample absorbance (p-polarized) was then directly used to evaluate $\langle P_2 \rangle$. However, from the work of Mansuripur, rigorous simulation (through Jones matrix analysis) of raw experimental data shows that the simple Graf analysis is not sufficient in the case of highly absorptive media.[26] The complex refractive index must be rigorously included to accurately determine $\langle P_2 \rangle$.

For illustration, a representative 0.95 μm thick guest/host sample of chromophore YLD_124 (2-[4-(3-{3-[2-(4-{bis-[2-(tert-butyl-dimethyl-silanyloxy)-ethyl]-amino}-phenyl)-vinyl]-5,5-dimethyl-cyclohex-2-enylidene}-propenyl)-3-cyano-5-phenyl-5-trifluoromethyl-5*H*-furan-2-ylidene]-malononitrile; 15% (w/w) in poly(methyl methacrylate) (PMMA) {$N = 1.2 \times 10^{20}$ molecules/cc}), was poled at $E_p = 50$ V/μm and analyzed. For the analysis models, all input parameters are fixed (the real and imaginary components of the refractive indices of the glass, ITO, and EO layers as well as their thicknesses) using experimentally determined values. In Figure 4, it is shown that the resulting experimental raw data can be fit well using the rigorous method assuming $\langle P_2 \rangle = 0.03$. However, the simple method fit, using Snell's law and Fresnel reflection approximations, is quite poor.

Because the rigorous analysis can be time-intensive, the variable angle polarization referenced absorbance spectroscopy (VAPRAS) method was recently developed by the Robinson and Dalton groups to improve accessibility. In the VAPRAS method, the data are analyzed in a similar manner to that of Graf, except that the angle dependence of the absorption of light polarized perpendicular to the poling axis (s-polarized), taken from the same sample, is used as a reference. Unlike p-polarized light, for the case where the light is s-polarized, the average absorbance does not depend upon ψ and the relation analogous to eq 4 can be written as

$$\langle \alpha_f(\tilde{\nu}) \rangle_s = \bar{\alpha}_f\{1 - \langle P_2 \rangle\} \tag{5}$$

Then, $\langle P_2 \rangle$ may be calculated directly from the data using the ratio of the absorbances for the s and p polarizations, such that

$$\frac{\langle \alpha_f(\tilde{\nu}) \rangle_p}{\langle \alpha_f(\tilde{\nu}) \rangle_s} = 1 + \sin^2 \theta \left(\frac{3\langle P_2 \rangle}{1 - \langle P_2 \rangle \eta(\tilde{\nu})^2} \right) \tag{6}$$

where $\eta(\tilde{\nu})$ is the complex refractive index of the EO layer at optical frequency $\tilde{\nu}$. This VAPRAS analysis method allows for much of the error associated with the simplified treatment to be canceled, removes the dependence upon the sample thickness, and appears to be less sensitive to fluctuations in the refractive index.

When the rigorous and VAPRAS methods are compared to $\langle P_2 \rangle$ derived from PAMC computer simulations, we see that the rigorous method gives a best fit for $\langle P_2 \rangle = 0.03$, the VAPRAS method yields $\langle P_2 \rangle = 0.036$, and the value determined from PAMC simulations is $\langle P_2 \rangle = 0.034$. The PAMC simulations were performed on a molecular ensemble of dipolar spheres ($\mu_0 = 24$ D) under the application of a poling field of $E_p = 100$ V/μm, assuming a dielectric permittivity value of $\varepsilon_0 = 1$. In a dielectric environment of $\varepsilon_0 \approx 3.5-4.0$, such as YLD_124 in

PMMA, these values correspond to $\mu_0 = 12$ D and $E_p = 50$ V/μm.[22] The sample studied here was found to have $r_{33} = 44 \pm 8$ pm/V, as measured by attenuated total reflection (ATR, $\lambda_{exp} = 1310$ nm). Work is in progress in our laboratories to use $\langle P_2 \rangle$ and ATR data along with PAMC simulations (which yield $\langle \cos^3(\theta) \rangle = 0.77 \langle P_2 \rangle^{1/2}$) to directly estimate effective β_{zzz} of a number of EO chromophores in the solid state.

Classes of OEO Materials Investigated. We have applied the above-mentioned theoretical methods successfully to traditional chromophore/polymer composite materials, chromophores incorporated into polymers, dendrimers, and dendronized polymers, and most recently, chromophores incorporated into chromophore-containing host materials, which we refer to as binary chromophore organic glasses (BCOGs).[27] In traditional chromophore/polymer composite materials, the two critical spatially anisotropic intermolecular electrostatic interactions are chromophore−chromophore dipolar interactions and nuclear repulsive (steric) interactions.[28] The chromophore shape is the factor that is most critical in optimizing electro-optic activity.[22] With covalently incorporated chromophores, covalent bond potentials play an additional important role in defining maximum achievable EO activity.[12] BCOGs represent a new family of OEO materials that exhibit very desirable EO and optical loss properties.[19,27,29,30] These materials exhibit very favorable free energies of mixing, permitting high chromophore number densities to be achieved without phase separation and accompanying scattering loss. Solvatochromic shifts are minimal with BCOGs. The spatially anisotropic interactions among the two types of chromophores can lead to improved $\langle \cos^3 \theta \rangle$ values. Finally, the higher ε values of BCOGs can lead to enhanced molecular first hyperpolarizabilities. Theory has provided a rationalization of the observed EO activity for each of these classes of materials and suggest a number of additional modifications (additional spatially anisotropic interactions) that can be made to further improved EO activity.

Material Thermal and Photostability

Thermal Stability. To realize materials that may be used in real-world EO devices, it is important to consider not only improved EO coefficients but also thermal and photochemical stability. The performance of devices operating at elevated temperatures must not degrade. Stability at elevated temperatures requires that the constituents of the material system (chromophore and host) be thermally robust and that acentric alignment be maintained. The thermal stability of chromophores and polymers depends upon fundamental chemical structures as well as purity.[31] Postpoling chromophore alignment stability depends upon the material glass transition temperature, T_g (rigidity of the material lattice). Much recent effort has been devoted to the development of lattice hardening (cross-linking) chemistries that are compatible with processing conditions. Two of the most recent and successful strategies are based on Diels−Alder cycloaddition "click chemistry"[29,32,33] and perfluorovinyl ether thermal cross-linking.[34,35] Recent reports reveal that chemical thermal stability and alignment stability can both be significantly improved through a combination of chromphore funtionalization and cross-linking.[36] Through the use of anthracene/acrylate Diels−Alder cross-linking to stabilize dendronized AJL8- (or YLD_156) type chromophores, long-term r_{33} stability at over 150 °C was realized. These materials were also able to withstand temperatures up to 230 °C for short periods.

Photostability. In addition to thermal stability, photostability has been a major concern for EO materials. It is generally expected that devices will function for 10 years at telecommunication power levels (e.g., 10 mW). Characterization of the relative photostability of materials has generally been accomplished by pump−probe measurements. Various models for photodegradation involving either one or multiple pathways have been used to analyze data.[37−39] It has proven useful to define a photostability figure-of-merit (FOM), B/σ, where B^{-1} is the probability of photodecay from the LUMO charge-transfer state of the chromophore and σ is the chromophore interband (charge-transfer) absorption coefficient.[40] This FOM is justified by the universal observation that the rate of photodegradation depends upon the separation of the pump wavelength from the absorption maximum of the chromophore charge-transfer transition. The dominant mechanism of photodecay appears to be absorption of light by the chromophore followed by excitation of oxygen dissolved in the material matrix, generation of a singlet oxygen, and attack of the singlet oxygen on selected sites along the π conjugation of the chromophore. Research has also shown that photostability FOM values for a given chromophore can be varied by 4−5 orders of magnitude as a function of chromophore and lattice modification, including the addition of singlet oxygen quenchers.[37,40,41] A photostability FOM value of B/σ, of greater than 250×10^{32} m^{-2}, is necessary to satisfy 10 years of survivability. Values with an order of magnitude higher have been achieved with chromophore modification and with packaging to exclude oxygen. Thus, packaging of OEO materials as well as OLED materials appears important for the most stringent device applications.

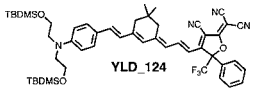

r_{33}/E_p poling efficiency		
	Au cathode	Au anode
Bare ITO	0.93+/-0.14	0.96+/-0.07
TiO_2	1.23+/-0.01	1.27+/-0.08

FIGURE 5. r_{33}/E_p values for 25% (w/w) YLD_124 in PMMA films cast on either bare ITO-coated glass or ITO-coated glass modified with a ~90 nm thick layer of TiO_2. Results for both forward and backward E_p biases are shown.

Materials Processing

Controlling Conductivity at Electrode/EO Material Interfaces. One factor that limits the maximum r_{33} that can be achieved is the maximum poling voltage that can be applied before dielectric breakdown occurs. In the low order limit, r_{33} is approximately linear with E_p (applied at optimum temperature). Therefore, the parameter r_{33}/E_p along with the maximum voltage that can be applied before breakdown occurs defines the maximum r_{33} that can be obtained from any given material. Materials that exhibit decreased resistivity during the poling process undergo dielectric breakdown under lower poling voltage (E_p). The newest EO materials including binary chromophore glasses and dendrimers all contain high chromophore densities. These high-activity materials show r_{33}/E_p values in the range of 3−5 but also are much more conductive than simple inert polymer (host)/chromophore (guest) materials. The development of methods to limit charge injection at the electrode EO material interfaces can help to increase the E_p that may be applied. Several methods have been used to accomplish similar goals in fields, such as organic field effect transistors[42] and photovoltaics.[43] Of these methods, metal oxide layers, such as TiO_2, and self-assembled dipolar monolayers are the most attractive for applications involving OEO materials because they can yield large interface effects, are easily fabricated on an ITO/glass surface, and can be made very thin and transparent. Preliminary experiments using sol−gel-processed TiO_2 films fabricated directly atop ITO electrodes show promising results. Figure 5 illustrates poling results comparing r_{33}/E_p values for guest/host composites of 25% (w/w) of the chromophore YLD_124 in PMMA.

Samples were poled on bare ITO substrates and substrates that were pretreated by deposition of an approximately 90 nm thick layer of TiO_2. Measurement of r_{33} values was performed using the ATR technique at $\lambda = 1310$ nm.[8] When the TiO_2 layer was used to modify the electrical properties of the ITO polymer interface, r_{33}/E_p is enhanced by 32%. Tests performed to compare poling efficiency when the poling bias was reversed (gold electrode is used as the anode) revealed very little dependence of r_{33}/E_p on the poling bias used. TiO_2 is an n-type semiconductor (hole-blocking layer). However, under the processing conditions used here, the TiO_2 layer is estimated to have a resistivity of 2×10^{11} Ω cm and dielectric constant of approximately $\varepsilon = 40$. These data suggest that, in this application, the TiO_2 layer acts to effectively reduce the injection/transport of both holes and electrons. Studies are currently underway to determine the effects of different metal oxide dielectric layers as well as the use of dipolar monolayers for interface modification. A number of hybrid polymer/sol−gel waveguide devices have been demonstrated to date that take advantage of these blocking layer effects to yield improved poling efficiency and reduced V_π.[44,45]

Laser-Assisted Electric Field Poling (LAPEP) of Binary Chromophore Organic Glasses (BCOGs). In addition to electric field poling, LAPEP techniques have been introduced. Through the addition of a polarized optical field, enhancements in r_{33} of up to a factor of 2.5 can be achieved. The use of a polarized optical field to influence the order of DR-1-type azo-dyes has been previously described.[46] Photo-induced trans−cis−trans isomerization of the azo-dye allows the dye enough mobility to rotate into an orientation where its transition dipole is perpendicular to the electric field vector of the laser light, inducing net polar order.[47] BCOGs have demonstrated enhanced order and potential cooperative effects related to intermolecular electrostatic interactions between the guest and host.[27] Therefore, the enhanced order produced in a photo-addressable host material may be transferred to a nonphoto-addressable guest contained within the matrix.[48] When the host is ordered using the polarized optical field, a spatially anisotropic lattice is created. The electrostatic interactions between the guest and host serve to enhance the alignment of the guest chromophore in two dimensions. The overall lattice symmetry is then further reduced by the addition of a large electric poling field oriented perpendicular to the optical field polarization (parallel to the chromophore alignment), to achieve enhanced acentric alignment of the guest chromophore.

Conclusion and Outlook

To have the greatest commercial impact, it is likely that the activity of OEO materials will have to be improved to values in the range of 500−1000 pm/V. Because of the advances being made in theory-inspired design of materials and efforts to address problems caused by material conductivity, this goal

appears achievable. The current thermal and photochemical stability for OEO materials appears adequate, as well as optical loss. OEO materials afford many processing advantages and appear to be compatible with a wide range of materials. Recent success in integrating OEO materials with silicon photonic circuitry appears to be particularly important because silicon photonics leads to significant size reduction for photonic circuitry (a feature very attractive for chipscale integration of electronics and photonics). Moreover, silicon photonics permits leveraging the substantial investment in complementary metal oxide semiconductor (CMOS) electronic circuitry foundries.

The authors gratefully acknowledge financial support provided by the National Science Foundation (DMR-0551020 and DMR-0120967) and the Air Force Office of Scientific Research (F49620-1-0110-P000). Helpful discussions and technical assistance provided by members of the Robinson, Hochberg, Prezhdo, Scherer, and Jen research groups are also gratefully acknowledged, as well as many helpful discussions with Professors Bruce Robinson (UW), Michael Hochberg (UW), Oleg Prezhdo (UW), Axel Scherer (Cal Tech), and Alex Jen (UW).

BIOGRAPHICAL INFORMATION

Philip A. Sullivan received his B.S. (Honors) degree in chemistry at Montana State University in Bozeman under the instruction of Cynthia McClure. He received his Ph.D. in chemistry and nanotechnology in 2007 from University of Washington, working with Larry Dalton. His dissertation was focused on the synthesis and characterization of novel nanostructured organic materials for second-order nonlinear optical applications. He is currently a Research Assistant Professor of Chemistry at the University of Washington.

Larry R. Dalton received a B.S. in chemistry and mathematics from the Honors College of Michigan State University in 1965, a M.S. in chemistry in 1966 working with James Dye, and A.M. and Ph.D. degrees in chemistry from Harvard University in 1971 working with Alvin Kwiram. He is the recipient of the Richard C. Tolman Medal of the American Chemical Society (Southern California Section), the 2003 Chemistry of Materials Award of the American Chemical Society, the 2006 IEEE/LEOS William Streifer Scientific Achievement Award, and the 2008 Lifetime Achievement Award, SPIE—International Society of Optics and Photonics. He is the B. Seymour Rabinovitch Chair Professor of Chemistry and the Director of the National Science Foundation Science and Technology Center on Materials and Devices for Information Technology Research at the University of Washington.

FOOTNOTES

*To whom correspondence should be addressed. E-mail: dalton@chem.washington.edu.

REFERENCES

1 Singer, K. D.; Kuzyk, M. G.; Sohn, J. E. Second-order nonlinear-optical processes in orientationally ordered materials: Relationship between molecular and macroscopic properties. *J. Opt. Soc. Am. B* **1987**, *4* (6), 968–976.

2 Isborn, C. M.; Leclercq, A.; Vila, F. D.; Dalton, L. R.; Bredas, J. L.; Eichinger, B. E.; Robinson, B. H. Comparison of static first hyperpolarizabilities calculated with various quantum mechanical methods. *J. Phys. Chem. A* **2007**, *111* (7), 1319–1327.

3 Dalton, L. R. Rational design of organic electro-optic materials. *J. Phys.: Condens. Matter* **2003**, *15* (20), R897–R934.

4 Liao, Y.; Eichinger, B. E.; Firestone, K. A.; Haller, M.; Luo, J.; Kaminsky, W.; Benedict, J. B.; Reid, P. J.; Jen, A. K. Y.; Dalton, L. R.; Robinson, B. H. Systematic study of the structure−property relationship of a series of ferrocenyl nonlinear optical chromophores. *J. Am. Chem. Soc.* **2005**, *127* (8), 2758–2766.

5 Davidson, E. R.; Eichinger, B. E.; Robinson, B. H. Hyperpolarizability: Calibration of theoretical methods for chloroform, water, acetonitrile, and *p*-nitroaniline. *Opt. Mater.* **2006**, *29*, 360.

6 Takimoto, Y.; Isborn, C. M.; Eichinger, B. E.; Rehr, J. J.; Robinson, B. H. Frequency and solvent dependence of nonlinear optical properties of molecules. *J. Phys. Chem. C* **2008**, *112*, 8016–8021.

7 Oudar, J. L.; Chemla, D. S. Hyperpolarizabilities of the nitroanilines and their relations to the excited state dipole moment. *J. Chem. Phys.* **1977**, *66* (6), 2664–2668.

8 Davies, J. A.; Elangovan, A.; Sullivan, P. A.; Olbricht, B. C.; Bale, D. H.; Ewy, T. R.; Isborn, C. M.; Eichinger, B. E.; Robinson, B. H.; Reid, P. J.; Li, X.; Dalton, L. R. Rational enhancement of second-order nonlinearity: Bis-(4-methoxyphenyl)heteroaryl-amino donor-based chromophores: Design, synthesis, and electrooptic activity. *J. Am. Chem. Soc.* **2008**, *130* (32), 10565–10575.

9 Dalton, L. R.; Sullivan, P. A.; Bale, D. H.; Olbricht, B. C. Theory-inspired nanoengineering of photonic and electronic materials: Noncentrosymmetric charge-transfer electro-optic materials. *Solid-State Electron.* **2007**, *51*, 1263–1277.

10 Clays, K.; Persoons, A. Hyper-Rayleigh scattering in solution. *Rev. Sci. Instrum.* **1992**, *63* (6), 3285–3289.

11 Firestone, K. A.; Reid, P.; Lawson, R.; Jang, S.-H.; Dalton, L. R. Advances in organic electro-optic materials and processing. *Inorg. Chim. Acta* **2004**, (357), 3957–3966.

12 Sullivan, P. A.; Rommel, H.; Liao, Y.; Olbricht, B. C.; Akelaitis, A. J. P.; Firestone, K. A.; Kang, J. W.; Luo, J.; Davies, J. A.; Choi, D. H.; Eichinger, B. E.; Reid, P. J.; Chen, A.; Jen, A. K. Y.; Robinson, B. H.; Dalton, L. R. Theory-guided design and synthesis of multichromophore dendrimers: An analysis of the electro-optic effect. *J. Am. Chem. Soc.* **2007**, *129* (24), 7523–7530.

13 Kinnibrugh, T.; Bhattacharjee, S.; Sullivan, P.; Isborn, C.; Robinson, B. H.; Eichinger, B. E. Influence of isomerization on nonlinear optical properties of molecules. *J. Phys. Chem. B* **2006**, *110*, 13512–13522.

14 Ma, H.; Chen, B.; Sassa, T.; Dalton, L. R.; Jen, A. K.-Y. Highly efficient and thermally stable nonlinear optical dendrimer for electrooptics. *J. Am. Chem. Soc.* **2001**, *123* (5), 986–987.

15 Gopalan, P.; Katz, H. E.; McGee, D. J.; Erben, C.; Zielinski, T.; Bousquet, D.; Muller, D.; Grazul, J.; Olsson, Y. Star-shaped azo-based dipolar chromophores: Design, synthesis, matrix compatibility, and electro-optic activity. *J. Am. Chem. Soc.* **2004**, *126* (6), 1741–1747.

16 Luo, J.; Haller, M.; Li, H.; Tang, H.-Z.; Jen, A. K.-Y.; Jakka, K.; Chou, C.-H.; Shu, C.-F. A side-chain dendronized nonlinear optical polyimide with large and thermally stable electrooptic activity. *Macromolecules* **2004**, *37* (2), 248–250.

17 Luo, J.; Liu, S.; Haller, M.; Liu, L.; Ma, H.; Jen, A. K.-Y. Design, synthesis, and properties of highly efficient side-chain dendronized nonlinear optical polymers for electro-optics. *Adv. Mater.* **2002**, *14* (23), 1763–1768.

18 Facchetti, A.; Annoni, E.; Beverina, L.; Morone, M.; Zhu, P.; Marks, T. J.; Pagani, G. A. Very large electro-optic responses in H-bonded heteroaromatic films grown by physical vapor deposition. *Nat. Mater.* **2004**, *3* (12), 910–917.

19 Kim, T.-D.; Kang, J.-W.; Luo, J.; Jang, S.-H.; Ka, J.-W.; Tucker, N.; Benedict, J. B.; Dalton, L. R.; Gray, T.; Overney, R. M.; Park, D. H.; Herman, W. N.; Jen, A. K. Y. Ultralarge and thermally stable electro-optic activities from supramolecular self-assembled molecular glasses. *J. Am. Chem. Soc.* **2007**, *129* (3), 488–489.

20 Makowska-Janusik, M.; Reis, H.; Papadopoulos, M. G.; Economou, I. G.; Zacharopoulos, N. Molecular dynamics simulations of electric field poled nonlinear optical chromophores incorporated in a polymer matrix. *J. Phys Chem. B* **2004**, *108* (2), 588–596.

21 Wang, C. H. Effects of the orientational pair correlation on second order nonlinear optical coefficients. *J. Chem. Phys.* **1993**, *98* (4), 3457–3462.

22 Rommel, H.; Robinson, B. Orientation of electro-optic chromophores under poling conditions: A spheroidal model. *J. Phys. Chem. C* **2007**, *111* (50), 18765–18777.

23 Bartke, J.; Hentschke, R. Dielectric properties and the ferroelectric transition of the Stockmayer-fluid via computer simulation. *Mol. Phys.* **2006**, *104* (19), 3057–3068.

24 Onsager, L. Electric moments of molecules in liquids. *J. Am. Chem. Soc.* **1936**, *58*, 1486–1493.

25 Graf, H. M.; Oliver, Z.; Anthony, J. E.; Dietrich, H. The polarized absorption spectroscopy as a novel method for determining the orientational order of poled nonlinear optical polymer films. *J. App. Phys.* **1994**, *75* (7), 3335–3339.

26 Mansuripur, M. Analysis of multilayer thin-film structures containing magneto-optic and anisotropic media at oblique incidence using 2 × 2 matrices. *J. Appl. Phys.* **1990**, *67* (10), 6466–6475.

27 Pereverzev, Y. V.; Gunnerson, K. N.; Prezhdo, O. V.; Sullivan, P. A.; Liao, Y.; Olbricht, B. C.; Akelaitis, A. J. P.; Jen, A. K. Y.; Dalton, L. R. Guest−host cooperativity in organic materials greatly enhances the nonlinear optical response. *J. Phys. Chem. C* **2008**, *112* (11), 4355–4363.

28 Dalton, L. R.; Harper, A. W.; Robinson, B. H. The role of London forces in defining noncentrosymmetric order of high dipole moment−high hyperpolarizability chromphores in electrically poled polymeric thin films. *Proc. Natl. Acad. Sci. U.S.A.* **1997**, *94* (10), 4842–4847.

29 Kim, T.-D.; Luo, J.; Ka, J.-W.; Hau, S.; Tian, Y.; Shi, Z.; Tucker, N. M.; Jang, S.-H.; Kang, J.-W.; Jen, A. K. Y. Ultralarge and thermally stable electro-optic activities from Diels−Alder crosslinkable polymers containing binary chromophore systems. *Adv. Mater.* **2006**, *18* (22), 3038–3042.

30 Kim, T.-D.; Luo, J.; Cheng, Y.-J.; Shi, Z.; Hau, S.; Jang, S.-H.; Zhou, X. H.; Tian, Y.; Polishak, B.; Huang, S.; Ma, H.; Dalton, L. R.; Jen, A. K.-Y. Binary chromophore systems in nonlinear optical dendrimers and polymers for large electro-optic activities. *J. Phys. Chem. C* **2008**, *112* (21), 8091–8098.

31 Cho, M. J.; Choi, D. H.; Sullivan, P. A.; Akelaitis, A. J. P.; Dalton, L. R. Recent progress in second-order nonlinear optical polymers, dendrimers. *Prog. Polym. Sci.* **2008**, *33*, 1013–1058.

32 Sullivan, P. A.; Olbricht, B. C.; Akelaitis, A. J. P.; Mistry, A. A.; Liao, Y.; Dalton, L. R. Tri-component Diels−Alder polymerized dendrimer glass exhibiting large, thermally stable, electro-optic activity. *J. Mater. Chem.* **2007**, *17* (28), 2899–2903.

33 Luo, J.; Haller, M.; Li, H.; Kim, T.-D.; Jen, A. K.-Y. Highly efficient and thermally stable electro-optic polymer from a smartly controlled crosslinking process. *Adv. Mater.* **2003**, *15* (19), 1635–1638.

34 Budy, S. M.; Suresh, S.; Spraul, B. K.; Smith, D. W. High-temperature chromophores and perfluorocyclobutyl copolymers for electro-optic applications. *J. Phys. Chem. C* **2008**, *112*, 8099–8104.

35 Ma, H.; Liu, S.; Luo, J.; Suresh, S.; Liu, L.; Kang, S. H.; Haller, M.; Sassa, T.; Dalton, L. R.; Jen, A. K.-Y. Highly efficient and thermally stable electro-optical dendrimers for photonics. *Adv. Funct. Mater.* **2002**, *12* (9), 565–574.

36 Shi, Z.; Luo, J.; Huang, S.; Zhou, X. H.; Kim, T.-D.; Cheng, Y.-J.; Polishak, B. M.; Younkin, T. R.; Block, B. A.; Jen, A. K.-Y. Reinforced site isolation leading to remarkable thermal stability and high electro-optic acitvities in cross-linked nonlinear optical dendrimers. *Chem. Mater.* **2008**, *20*, 6372–6377.

37 Galvan-Gonzalez, A.; Canva, M.; Stegeman, G. I.; Twieg, R.; Kowalczyk, T. C.; Lackritz, H. S. Effect of temperature and atmospheric environment on the photodegradation of disperse red 1-type polymers. *Opt. Lett.* **1999**, *24* (23), 1741–1743.

38 Galvan-Gonzalez, A.; Canva, M.; Stegeman, G. I.; Sukhomlinova, L.; Twieg, R. J.; Chan, K. P.; Kowalczyk, T. C.; Lackritz, H. S. Photodegradation of azobenzene nonlinear optical chromophores: The influence of structure and environment. *J. Opt. Soc. Am. B* **2000**, *17* (12), 1992–2000.

39 Galvan-Gonzalez, A.; Belfield, K. D.; Stegeman, G. I.; Canva, M.; Marder, S. R.; Staub, K.; Levina, G.; Twieg, R. J. Photodegradation of selected π-conjugated electrooptic chromophores. *J. Appl. Phys.* **2003**, *94* (1), 756–763.

40 Rezzonico, D.; Jazbinsek, M.; Gunter, P.; Bosshard, C.; Bale, D. H.; Liao, Y.; Dalton, L. R.; Reid, P. J. Photostability studies of π-conjugated chromophores with resonant and nonresonant light excitation for long-life polymeric telecommunication devices. *J. Opt. Soc. Am. B* **2007**, *24* (9), 2199–2207.

41 Cheng, Y.-J.; Luo, J.; Huang, S.; Zhou, X. H.; Shi, Z.; Kim, T.-D.; Bale, D. H.; Takahashi, S.; Yick, A.; Polishak, B. M.; Jang, S.-H.; Dalton, L. R.; Reid, P. J.; Steier, W. H.; Jen, A. K.-Y. Donor−acceptor thiolated polyenic chromophores exhibiting large optical nonlinearity and excellent photostability. *Chem. Mater.* **2008**, *20*, 5047–5054.

42 Byrne, P. D.; Facchetti, A.; Marks, T. J. High-performance thin-film transistors from solution-processed cadmium selenide and a self-assembled multilayer gate dielectric. *Adv. Mater.* **2008**, *20* (12), 2319–2324.

43 Kim, J. Y.; Kim, S. H.; Lee, H.-H.; Lee, K.; Ma, W.; Gong, X.; Heeger, A. J. New architecture for high-efficiency polymer photovoltaic cells using solution-based titanium oxide as an optical spacer. *Adv. Mater.* **2006**, *18*, 572–576.

44 Enami, Y.; Derose, C. T.; Mathine, D.; Loychik, C.; Greenlee, C.; Norwood, R. A.; Kim, T.-D.; Luo, J.; Tian, Y.; Jen, A. K.-Y.; Peyghambarian, N. Hybrid polymer/sol−gel waveguide modulators with exceptionally large electro-optic coefficients. *Nat. Photonics* **2007**, *1*, 180–185.

45 Enami, Y.; Mathine, D.; Derose, C. T.; Norwood, R. A.; Luo, J.; Jen, A. K.-Y.; Peyghambarian, N. Hybrid cross-linkable polymer/sol−gel waveguide modulators with 0.65 V half wave voltage at 1550 nm. *Appl. Phys. Lett.* **2007**, *91*, 093505.

46 Tawa, K.; Kamada, K.; Kiyohara, K.; Ohta, K.; Yasumatsu, D.; Sekkat, Z.; Kawata, S. Photoinduced Reorientation of azo dyes bonded to polyurethane studied by polarized FT-IR spectroscopy. *Macromolecules* **2001**, *34*, 8232–8238.

47 Mayer, S. G.; Thomsen, C. L.; Philpott, M. P.; Reid, P. J. The solvent-dependent isomerization dynamics of 4-(dimethylamino) azobenzene (DMAAB) studied by subpicosecond pump-probe spectroscopy. *Chem. Phys. Lett.* **1999**, *314*, 246–254.

48 Olbricht, B. C.; Sullivan, P. A.; Wen, G.-A.; Mistry, A.; Davies, J. A.; Ewy, T. R.; Eichinger, B. E.; Robinson, B. H.; Reid, P. J.; Dalton, L. R. Laser-assisted poling of binary chromophore materials. *J. Phys. Chem. C* **2008**, *112* (21), 7983–7988.